Jurnal
Teknologi

Full Paper

APPLICATION OF IMAGE DIGITAL PROCESSING TO EVALUATE ACCURACY IN PREDICTING ROCK FRAGMENTATION INDUCED BY BLASTING

Supandi Sujatono*

Department of Mining Engineering, Institut Teknologi Nasional Yogyakarta, Yogyakarta, Indonesia

Article history
Received
17 Juy 2023
Received in revised form
10 August 2023
Accepted
1 January 2024
Published Online
23 June 2024

*Corresponding author
supandi@itny.ac.id

Graphical abstract

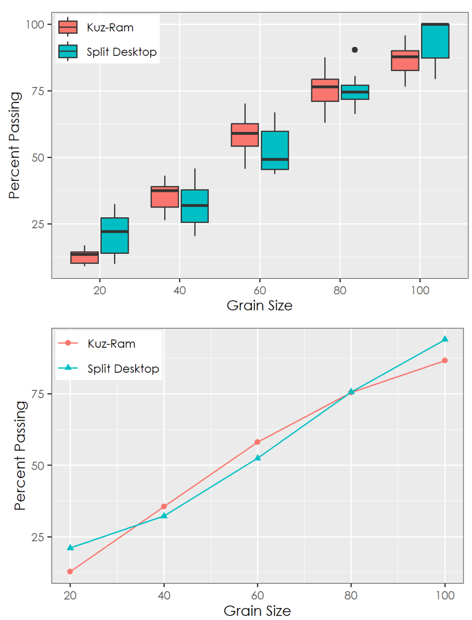

Abstract

Predicting rock fragmentation induced by blasting operation is important in order to evaluate the success of blasting operation. It is necessary to select a method that is in accordance with the characteristics of geological condition and rock mass so that it can quickly provide accurate information. This study aims to evaluate whether Kuz-Ram model is accurate enough in predicting fragmentation of andesite. The analysis was carried out statistically by comparing the andesite fragmentation based on theoretical calculation method by Kuz-Ram model to the fragmentation based on image analysis method by Split Desktop which represents the actual field condition. The data were obtained from 30 blasting operations on andesite. The analysis result shows that the fragmentation based on the theoretical calculation using Kuz-Ram model is not significantly different from the fragmentation based on Split Desktop. The maximum error of percent passing predicted by Kuz-Ram model is around 7% with an average error of 4.94%. Based on the result, calculation using Kuz-Ram theory can be performed to predict fragmentation of andesite.

Keywords: Fragmentation, Kuz-Ram, Split Desktop, andesite, blasting

1.0 INTRODUCTION

Fragmentation prediction using Kuz-Ram model has been widely used because it considers rock properties and rock factor [1]. However, Kuz-Ram model has not considered timing effect and upper, therefore, it is necessary to evaluate Kuz-Ram model on every characteristic of geological condition [2]. The Kuznetsov-Cunningham-Ouchterlony (KCO) model predicts fragmentation by using an approach to rock properties and blast charge [3, 4]. Even though it is quite detailed in predicting fragmentation, in the parameters, every change of blast design must be made; therefore, for a certain condition, it is not applicable. Stereophotogrammetric method produces a fairly good accuracy on identification of coarse material although it has not been numerically quantifiable [5].

Fragmentation analysis method by digitization using Split Desktop has a quite better accuracy than theoretical calculation using Kuz-Ram model [6]. The coefficient determination (R^2) of 80% indicates that the calculation of limestone fragmentation based on Split Desktop and Kuz-Ram are relatively the same. Kuz-Ram is quite valid for predicting fragmentation in quarry based on Split Desktop based image [7]. The result of fragmentation analysis on granite using Split Desktop is in line with fragmentation prediction using Kuz-Ram model [8].

Adjustment of Kuz-Ram parameter in predicting fragmentation must be carried out by considering detailed geological condition and rock mass [9, 10, 11]. Type of stemming material also affects rock fragmentation [12, 13]. Conventional blasting method produces 16% more fines compared to the other methods [14]. Cast distance depends on bench height and rock fragmentation. The higher the bench, the farther the cast length on the same fragmentation [15]. Identification of material in field, including broken muck induced by blasting, may use an aerial photographic approach [16].

The increase in size distribution of blasted rocks does not only depend on the increase in spacing, opening, roughness, persistence, waviness of discontinuities, as well as P-wave velocity and uniaxial compressive strength (UCS) of intact rock, but also the increase in discontinuity angle with the bench face of blasting block [3]. A linear form of the joint spacing and joint orientation descriptions accounts for the rock structure. The non-dimensional ratio to the burden is used to write the spacing of joints [17]. Based on the coefficient determination (R^2), artificial neural network (ANN) and imperialism competitive algorithm (ICA) were compared for prediction of fragmentation. In order to obtain the desired percentile sizes in the range where the data are thought to be representative of the muck-pile fragmentation, approximately 10-90% passing, the size distributions have been interpolated [18]. Kuz-Ram model, which combines the blast design parameters and the rock fragment size distribution, is typically used to quantify the size of rock fragmentation prior to drilling and blasting [19]. By using Monte Carlo simulation, we can better understand how rock mass and explosive properties affect rock fragmentation due to blasting, and have more faith in these empirical models [20]. Prediction model based on rock engineering systems (RES) that has higher R^2 and lower RMSE outperforms the other models [21, 22].

The number of boulders is one of the criteria for the success of blasting operation. The estimated number of boulders may be obtained from a fragmentation model by Kuz-Ram. Rock factor is one of the factors involved in estimating the number of boulders by Kuz-Ram model. The way to quantify rock factor is by a rock mass weighting, namely blastability index (BI). Rock mass has an important role in blasting design for the expected fragmentation. The rock mass assessment will be a correction factor for physical and mechanical properties of the rock. When rocks have same physical and mechanical properties but different rock mass, then the blasting design will be different. When the blasting design is the same, it will produce different fragmentation values. A series of parameters, including rock mass description (RMD), joint plane spacing (JPS), joint plane orientation (JPO), specific gravity influence (SGI), and hardness (HD), are used to calculate blastability index [23], as stated in Eq. (1).

$$BI = 0.5\,(RMD + JPS + JPO + SGI + HD) \quad (1)$$

Lilly [23] proposed a method for determining rock factor (RF) which is relatively more precise. The rock factor is obtained from blastability index (BI) of the rock. According to Lilly [23], the relationship between rock factor and blastability index is Eq. (2):

$$RF = BI \times 0.12 \quad (2)$$

The average size of fragmentation induced by blasting can be estimated by using Kuznetsov [24] equation as follows (Eq. (3)):

$$X = RF\left(\frac{V}{Q}\right)^{0.8} Q^{0.17}\left(\frac{E}{115}\right)^{-0.63} \quad (3)$$

X = Average size of fragmentation (cm)
RF = Rock factor
V = Volume of blasted rock (m^3)
Q = Explosive charge per blast hole (kg)
E = Relative weight strength of explosive (ANFO = 100)

In order to determine the percentage of boulder due to blasting, uniformity index (Eq. (4)) and characteristic size (Eq. (5)) need to be determined first. Once they are known, the percentage of boulder in Eq. (6) can be calculated. Ouchterlony and Sanchidrián [25] reviewed the development of prediction equations for blast fragmentation as presented in Table 1.

$$n = \left(2.2 - 14\frac{B}{D}\right)\left(1 - \frac{W}{B}\right)\left[1 + \frac{\left(\frac{S}{B}-1\right)}{2}\right]\left(\frac{L}{H}\right) \quad (4)$$

n = Uniformity index
B = Burden
D = Blast-hole diameter
W = Standard deviation of drilling accuracy
S = Spacing
L = Charge length above grade level
H = Bench height

$$Xc = \frac{X}{(0.693)^{\frac{1}{n}}} \quad (5)$$

Xc = Characteristic size (cm)
X = Average size of fragmentation (cm)
n = Uniformity index

$$R_x = 100\left[e^{-\left(\frac{x}{Xc}\right)^n}\right] \quad (6)$$

Rx = Percentage of material retained on sieve (%)
x = Sieve size (cm)
Xc = Characteristic size (cm)
n = Uniformity index

In calculating rock factor, Kuz-Ram does not account for the presence of water in blast hole. The presence of water in blast hole may affect blasting energy. Blasting index only pays attention to rock mass description (RMD), joint plane spacing (JPS), joint plane orientation (JPO), specific gravity influence (SGI), and hardness (HD). The factor that is not considered in prediction by Kuz-Ram model is blast delay time as a parameter that affects fragmentation induced by blasting. This study used 3 delay times (2 ms, 6 ms, and 8 ms) to improve the fragmentation distribution outcome. In the prediction, the amount of explosive charge is considered the same for each hole, while in the application in the field, the amount of explosive charge is different for each hole. Error when analyzing noise using desktop software may result in a lot of fragmentations not in accordance with the original sizes. The existing shadows can also cause noise.

Fragmentation depends on physical and mechanical properties of the rock, geological condition, and rock mass. These parameters are the main parameters in determining a blasting plan according to the expected fragmentation.

This study seeks to verify Kuz-Ram method in predicting rock fragmentation. The Kuz-Ram method is valid for predicting fragmentation of andesitic rocks. The factor of rock mass needs to be considered for obtaining a good accuracy. By considering the rock mass factor, the estimation of fragmentation using Kuz-Ram method remains relevant.

Table 1 Prediction equations for blast fragmentation

Name of Prediction Equation	Equation
Early fragmentation models	$x_{50} = f_1(rock)f_2(geometry)f_3(explosives)$
The first Kuz-Ram models	$n = \left(2.2 - 14\frac{B}{D}\right)\left(1 - \frac{W}{B}\right)\left[1 + \frac{\left(\frac{S}{B} - 1\right)}{2}\right]\left(\frac{L}{H}\right)$
Work by US Bureau of Mines and Chung and Katsabanis	$n = \ln\left(\frac{\ln 5}{\ln 2}\right) / \ln\left(\frac{x_{80}}{x_{50}}\right) = 0.842/\ln\left(\frac{x_{80}}{x_{50}}\right)$
The Julius Kruttschnitt Mineral Research Centre (JKMRC) models	$P_{(x)} = \begin{cases} 1 - e^{-\ln 10\left(\frac{x}{x_{90}}\right)^{n_{fines}}} & when\ x \le x_{90} \\ 1 - e^{-\ln 10\left(\frac{x}{x_{90}}\right)^{n_{coarse}}} & when\ x \ge x_{90} \end{cases}$
The extended Kuz-Ram model	$n = n_s\sqrt{\left(2 - \frac{30B}{D}\right)}\sqrt{\frac{\left(1 + \frac{S}{B}\right)}{2}}\left(1 - \frac{W}{B}\right)\left(\frac{L}{H}\right)^{0.3}\left(\frac{A}{6}\right)^{0.3} C(n)$
The Swebrec function	$P_{ExSwe} = \frac{1}{1 + a\left[\frac{\ln(x_{max}/x)}{\ln(x_{max}/x_{50})}\right]^b + (1 - a)\left(\frac{x_{max}/x - 1}{x_{max}/x_{50} - 1}\right)^c}$
The fragmentation-energy fan	$P(x,q) = P\left\{\left[\frac{\ln(x_0/x)}{\ln(q/q_0)} - \alpha_{100}\right]/(\alpha_{50} - \alpha_{100})\right\}$
A distribution-free blast model	$\frac{x_P}{L_c} = kk_2^h\left(\frac{\bar{\sigma}}{qeL_c^\lambda}\right)^k \quad with \quad \bar{\sigma} = \sigma_c^2/(2E)$

The various existing methods definitely consider geological aspect, rock mass, as well as physical and mechanical properties of rock. A change in these variables causes a change in the formula of fragmentation model. All the formulas from previous researchers have similarity in predicting fragmentation. Blasting design adjusts to geological condition and rock mass in determining the expected fragmentation.

2.0 METHODOLOGY

The study was conducted at the Warukin Formation which consists of sandstone, claystone, and coal units. Sedimentary rock has low hardness, and it will experience a degradation of mechanical properties when it is exposed [26]. The sandstone is composed of fine to coarse quartz minerals with a rupture angle of 53° [27]. There is hardly any presence of clay mineral in the claystone because the clay-sized material in the claystone is clay-sized quartz mineral [28]. About 15% of the clay mineral composition is kaolinite and 8% is illite [29], due to the provenance of the quartz mineral which is recycled orogen from older formation. Table 2 provides information about rock mass in the research area in general. Specifically, the rock hardness (Uniaxial Compressive Strength) of the studied andesite is 28 MPa in average.

The analysis phase begins with an introduction to the research area, technical data collection, fragmentation simulation using the Kuz-Ram model to obtain a particle size distribution curve, and image processing analysis using Split Desktop version 3.0. The data collection was carried out after blasting, with vertical and horizontal sampling (Figure 1). For vertical distribution, sampling was carried out from the lowest position to the highest. Samples were collected at the top, middle, and toe of the blasted area. Each area was considered to have a potential overlap of around 25%, in order to increase the accuracy of the analysis. Three photographs of slope sections represented one sample. For each blasting, sampling was carried out at least three times, and each sample collected was represented by three photographs.

Table 2 Rock mass in the research area

Parameter	Weighting
1. Rock mass description (RMD)	
1.1. Powdery/friable	10
1.2. Blocky	20
1.3. Totally massive	50
2. Join plane spacing (JPS)	
2.1. Close (space < 0.1 m)	10
2.2. Intermediate (space 0.1-1 m)	20
2.3. Wide (space >1 m)	50
3. Join plane orientation (JPO)	
3.1. Horizontal	10
3.2. Dip out of face	20
3.3. Strike normal to face	30
3.4. Dip into face	40
4. Specific gravity influence	SGI = 25 × Density – 50
5. Rock Strength (MPa)	28

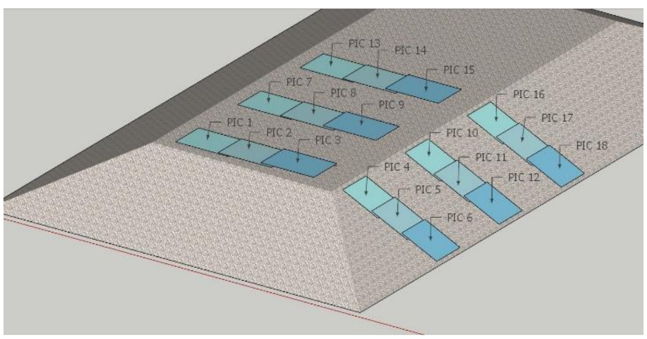

Figure 1 Vertical and horizontal sampling

Horizontal sampling was carried out along the blasting area at the top of it. At least three photographs were taken for each blast line, and three samples were collected horizontally. One sampling reported in the analysis is a composite of various samples. The various kinds of samples were expected to meet the need of samples so that the analysis result would be even more accurate.

Each sample used a ball, placed at the top and bottom of the photographs, as a parameter. Sampling was carried out perpendicular to the object. While sampling, flash was not used and the sun shadow was reduced.

The image analysis utilized the photographs taken in the field to be processed by the software. This software works by analyzing digital image to calculate particle-size distribution (PSD) of rock fragments. The data for this study were obtained from the monitoring on blasting activities, with the blasting design presented in Table 3, that have been carried out since the last one year.

Table 3 Blasting design

Blasting Geometry	Average
Burden	2.58 m
Space	3.51 m
Stemming	1.98 m
Column charge	4.01 m
Height of blast hole	6.00 m
Diameter of blast hole	76.20 mm

The blasting samples were collected throughout the course of eight distinct days. The blasting resulted in rock fragmentation with the observed grain sizes of 20 cm, 40 cm, 60 cm, 80 cm, and 100 cm. Table 4 shows the percent passing calculated by using two different methods, namely the Kuz-Ram theoretical calculation method and the image analysis method using Split Desktop.

Table 4 Percent passing based on Kuz-Ram and Split Desktop

Method	Grain Size	Blasting							
		1	2	3	4	5	6	7	8
Kuz-Ram	20 cm	14.14	8.94	9.70	16.83	13.12	15.16	10.37	13.79
	40 cm	43.02	26.27	28.80	41.13	38.30	36.80	32.17	38.11
	60 cm	70.10	45.55	49.68	62.56	62.97	56.67	55.69	61.46
	80 cm	87.46	62.92	67.75	78.19	80.94	72.20	74.76	78.82
	100 cm	95.76	76.55	81.11	88.23	91.50	83.16	87.37	89.61
Split Desktop	20 cm	24.24	13.61	14.05	27.33	19.84	27.15	9.80	32.33
	40 cm	32.79	24.68	20.19	40.71	36.79	30.96	25.74	45.74
	60 cm	51.87	46.53	43.61	59.60	66.88	45.24	45.53	60.16
	80 cm	80.57	66.30	75.54	73.46	90.28	72.22	70.54	75.94
	100 cm	100.00	79.33	100.00	83.43	100.00	100.00	100.00	88.56

The percent passing values by Kuz-Ram and Split Desktop were compared using ANOVA. ANOVA is a parametric method for testing differences between groups, and the model depends on research design. For a × b factorial design with replication as block, Eq. (7) represents the model [30].

$$Y_{ijk} = \mu + R_k + A_i + B_j + AB_{ij} + \epsilon_{ijk} \quad (7)$$

Y_{ijk} = Response variable of the k-th observation due to the i-th level of factor A and the j-th level of factor B

μ = Mean

R_k = k-th replication
A_i = Effect of the i-th level of factor A
B_j = Effect of the j-th level of factor B
AB_{ij} = Interaction effect between the i-th level of factor A and the j-th level of factor B
ϵ_{ijk} = Sample effect on the k-th replication for the i-th and the j-th level combination

Correction for percent passing by Kuz-Ram as theoretical method was obtained by building a regression model of the error value from Kuz-Ram, which is the difference between percent passing by Split Desktop as the actual value and percent passing by Kuz-Ram, based on grain size. Orthogonal polynomial was used to determine the regression order. In the polynomial regression model, the polynomial Y_x in X with m order is written as Eq. (8) [30]:

$$Y_x = A_0\xi_0 + A_1\xi_1 + \cdots + A_m\xi_m \quad (8)$$

Coefficient A is determined by calculating the sum of squares for each polynomial. For practical purpose, coefficient ξ can be determined based on Table 5 [30].

Table 5 Coefficient of orthogonal polynomial for k = 5

Polynomial	Scale of X					$\sum\xi_i^2$	λ
	1	2	3	4	5		
Linear	-2	-1	0	1	2	10	1
Quadratic	2	-1	-2	-1	2	14	1
Cubic	-1	2	0	-2	1	10	5/6
Quartic	1	-4	6	-4	1	17	35/12

3.0 RESULTS AND DISCUSSION

Table 6 presents summary statistics of percent passing by Kuz-Ram and Split Desktop, with the visualization of both data distribution shown in Figure 2. Percent passing values by Split Desktop appear to be relatively spread out (higher variance, wider range) compared to percent passing by Kuz-Ram. However, the averages are not that different.

To compare the percent passing, two-way ANOVA was applied, where the factors are method with two levels (Kuz-Ram and Split Desktop) and grain size with five levels (20 cm, 40 cm, 60 cm, 80 and 100 cm). Since the blastings were not carried out simultaneously on the same day, differences in the blasting operations might happen on the different days; and thus, blasting is considered as block in the model. The result of ANOVA is in Table 7.

With a significance level of 5%, percent passing obtained by Kuz-Ram method is not significantly different from percent passing obtained by Split Desktop. On the contrary, percent passing for different grain sizes, as well as the interaction between method and grain size, show significant differences. Figure 3 shows a visualization of the percent passing based on the two factors. To find out which part makes a difference, a post hoc test, Tukey's range test, was carried out, with the result in Table 8 and Figure 4.

Table 6 Summary statistics of percent passing

Method	Grain Size	Mean	Variance	Minimum	Maximum
Kuz-Ram	20 cm	12.76	7.88	8.94	16.83
	40 cm	35.58	35.10	26.27	43.02
	60 cm	58.09	62.21	45.55	70.10
	80 cm	75.38	60.09	62.92	87.46
	100 cm	86.66	37.59	76.55	95.76
Split Desktop	20 cm	21.04	63.78	9.80	32.33
	40 cm	32.20	74.46	20.19	45.74
	60 cm	52.43	76.03	43.61	66.88
	80 cm	75.61	52.63	66.30	90.28
	100 cm	93.92	76.64	79.33	100.00

Table 7 Two-way ANOVA on percent passing

	Degrees of Freedom	Sum of Squares	Mean Squares	F	p-value
Blasting	7	2136	305	11.383	3.11×10-9
Method	1	36	36	1.353	0.249
Grain size	4	56971	14243	531.308	< 2.00×10-16
Interaction	4	623	156	5.807	4.28×10-4
Residual	63	1689	27		

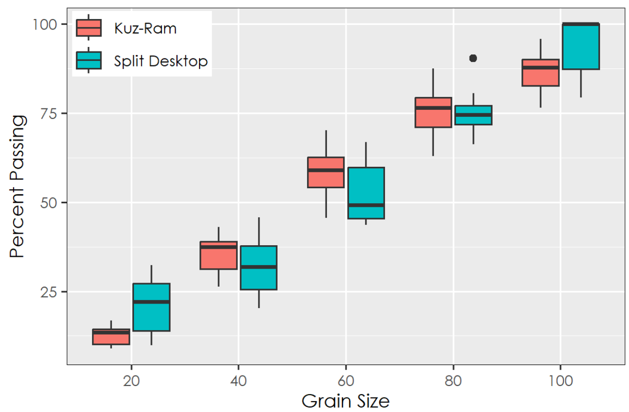

Figure 2 Boxplot of percent passing by Kuz-Ram and Split Desktop for each grain size

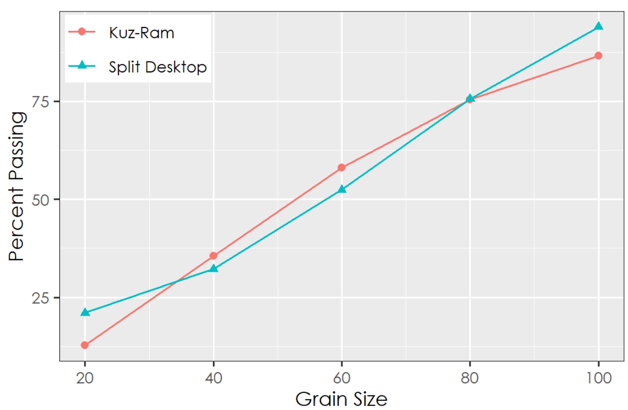

Figure 3 Interaction plot of method and grain size factors on percent passing

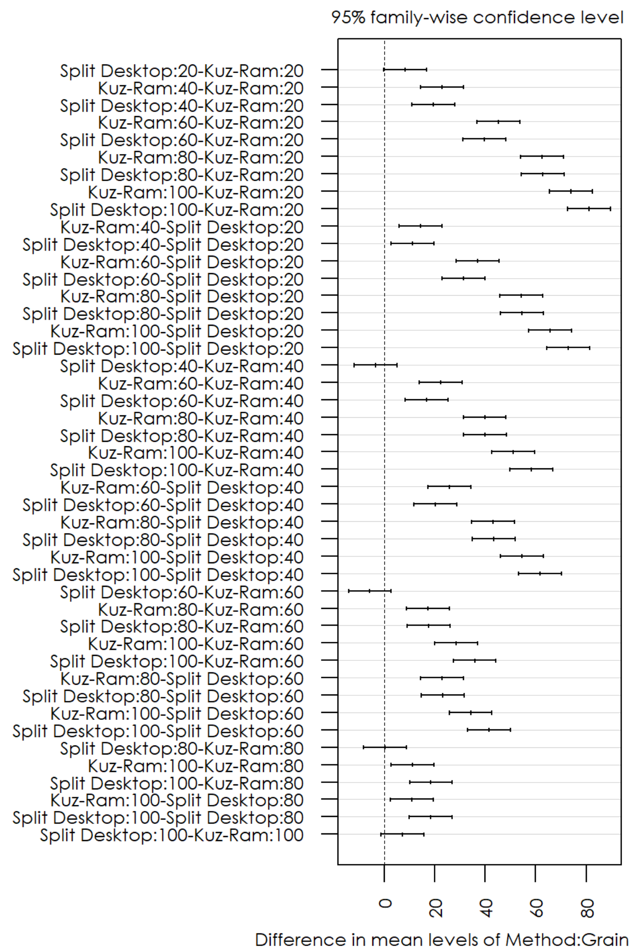

Figure 4 Plot of difference in percent passing based on method and grain size

Table 8 Tukey test on percent passing based on method and grain size

			Difference	Lower	Upper	p-value
Kuz-Ram 40 cm	-	Kuz-Ram 20 cm	22.820	14.330	31.310	0.000
Kuz-Ram 60 cm	-	Kuz-Ram 20 cm	45.330	36.840	53.820	0.000
Kuz-Ram 80 cm	-	Kuz-Ram 20 cm	62.623	54.133	71.113	0.000
Kuz-Ram 100 cm	-	Kuz-Ram 20 cm	73.907	65.417	82.397	0.000
Split 20 cm	-	Kuz-Ram 20 cm	8.288	-0.202	16.778	0.061
Split 40 cm	-	Kuz-Ram 20 cm	19.444	10.954	27.934	0.000
Split 60 cm	-	Kuz-Ram 20 cm	39.672	31.182	48.162	0.000
Split 80 cm	-	Kuz-Ram 20 cm	62.851	54.361	71.341	0.000
Split 100 cm	-	Kuz-Ram 20 cm	81.159	72.669	89.649	0.000
Kuz-Ram 40 cm	-	Split 20 cm	14.532	6.042	23.022	2.03×10-5
Kuz-Ram 60 cm	-	Split 20 cm	37.042	28.552	45.532	0.000
Kuz-Ram 80 cm	-	Split 20 cm	54.335	45.845	62.825	0.000
Kuz-Ram 100 cm	-	Split 20 cm	65.619	57.129	74.109	0.000
Split 40 cm	-	Split 20 cm	11.156	2.666	19.646	0.002
Split 60 cm	-	Split 20 cm	31.384	22.894	39.874	0.000
Split 80 cm	-	Split 20 cm	54.563	46.072	63.053	0.000
Split 100 cm	-	Split 20 cm	72.871	64.381	81.361	0.000
Kuz-Ram 60 cm	-	Kuz-Ram 40 cm	22.510	14.020	31.000	0.000
Kuz-Ram 80 cm	-	Kuz-Ram 40 cm	39.803	31.313	48.293	0.000
Kuz-Ram 100 cm	-	Kuz-Ram 40 cm	51.088	42.598	59.578	0.000
Split 40 cm	-	Kuz-Ram 40 cm	-3.375	-11.865	5.115	0.949
Split 60 cm	-	Kuz-Ram 40 cm	16.852	8.362	25.342	6.00×10-7
Split 80 cm	-	Kuz-Ram 40 cm	40.031	31.541	48.521	0.000
Split 100 cm	-	Kuz-Ram 40 cm	58.340	49.850	66.830	0.000
Kuz-Ram 60 cm	-	Split 40 cm	25.885	17.395	34.375	0.000

Table 8 Tukey test on percent passing based on method and grain size (continued)

			Difference	Lower	Upper	p-value
Kuz-Ram 80 cm	-	Split 40 cm	43.179	34.689	51.669	0.000
Kuz-Ram 100 cm	-	Split 40 cm	54.463	45.973	62.953	0.000
Split 60 cm	-	Split 40 cm	20.228	11.737	28.718	0.000
Split 80 cm	-	Split 40 cm	43.406	34.916	51.896	0.000
Split 100 cm	-	Split 40 cm	61.715	53.225	70.205	0.000
Kuz-Ram 80 cm	-	Kuz-Ram 60 cm	17.293	8.803	25.783	3.00×10-7
Kuz-Ram 100 cm	-	Kuz-Ram 60 cm	28.578	20.088	37.068	0.000
Split 60 cm	-	Kuz-Ram 60 cm	-5.658	-14.148	2.832	0.477
Split 80 cm	-	Kuz-Ram 60 cm	17.521	9.031	26.011	2.00×10-7
Split 100 cm	-	Kuz-Ram 60 cm	35.830	27.340	44.320	0.000
Kuz-Ram 80 cm	-	Split 60 cm	22.951	14.461	31.441	0.000
Kuz-Ram 100 cm	-	Split 60 cm	34.236	25.746	42.726	0.000
Split 80 cm	-	Split 60 cm	23.179	14.689	31.669	0.000
Split 100 cm	-	Split 60 cm	41.488	32.997	49.978	0.000
Kuz-Ram 100 cm	-	Kuz-Ram 80 cm	11.285	2.795	19.775	0.002
Split 80 cm	-	Kuz-Ram 80 cm	0.228	-8.262	8.718	1.000
Split 100 cm	-	Kuz-Ram 80 cm	18.536	10.046	27.026	0.000
Kuz-Ram 100 cm	-	Split 80 cm	11.057	2.567	19.547	0.002
Split 100 cm	-	Split 80 cm	18.309	9.819	26.799	1.00×10-7
Split 100 cm	-	Kuz-Ram 100 cm	7.252	-1.238	15.742	0.158

The p-value in Table 8 and the difference in Figure 4 show that with a significance level of 5%, different grain sizes in the same method have significantly different percent passing, while the same grain size in the different methods have non-significantly different passing percent. Figure 5 summarizes the differences. The line in Figure 5 indicates similarity in the percent passing value, hence, the levels that are not connected by the line show that there is a significant difference in the percent passing.

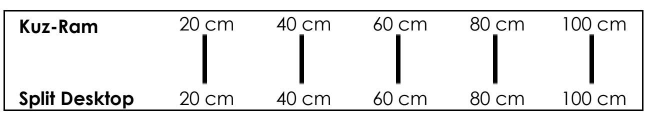

Figure 5 Summary of the difference test result on passing percent with the factors of method and grain size

Percent passing by Split Desktop was considered as actual data because it was obtained directly from field, while percent passing by Kuz-Ram method was obtained from the model prediction. The percent passing by Kuz-Ram was calibrated by constructing a regression model of the error values produced by Kuz-Ram method based on grain size as the factor. The regression order was determined through orthogonal polynomial with the result in Table 9.

Based on the p-value in Table 9, with a significance level of 5%, the appropriate regression order is second order, so the regression model is quadratic (Figure 6). Thus, the calibration model is as follows:

$$Correction = 0.0081\ Grain\ size^2 - 0.9683\ Grain\ size + 23.659$$

Table 9 Orthogonal polynomial

	Degrees of Freedom	Sum of Squares	Mean Squares	F	p-value
Grain size	4	1245.40	311.30	6.844	3.52×10-04
Linear	1	1.90	1.90	0.041	0.840
Quadratic	1	1185.30	1185.30	26.055	1.17×10-05
Cubic	1	54.40	54.40	1.195	0.282
Quartic	1	3.90	3.90	0.085	0.772
Residual	35	1592.20	45.50		

According to the model, the correction values for percent passing by Kuz-Ram based on grain size are in Table 10.

The errors produced by Kuz-Ram method in the same grain size have a wide range (Figure 6). This could be due to blasting factor since there is the effect of blasting on percent passing (Table 7). As additional information, Fig. 6 illustrates the difference in percent passing based on blasting according to Tukey test result.

Table 10 Correction for percent passing by Kuz-Ram

Grain Size	Correction
20 cm	7.533
40 cm	-2.113
60 cm	-5.279
80 cm	-1.965
100 cm	7.829

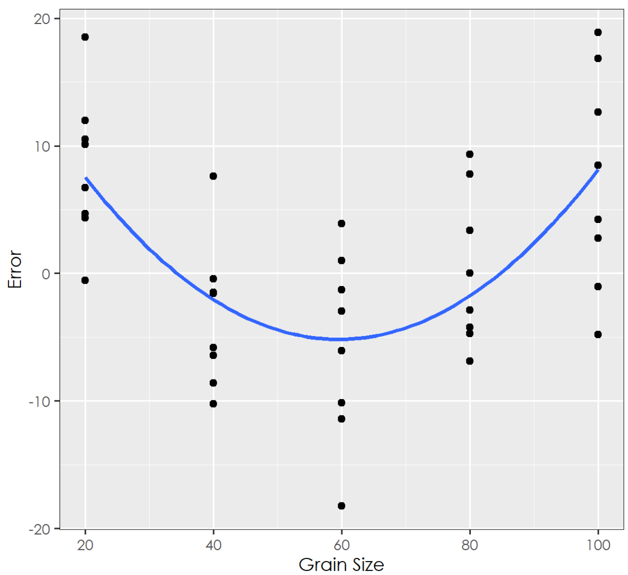

Figure 6 Plot of error produced by Kuz-Ram method against grain size forms a quadratic pattern (blue line)

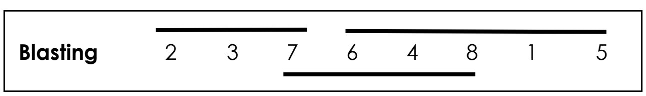

Figure 7 Summary of the difference test result on passing percent with the factor of blasting

The blasting in Figure 7 has been sorted from the lowest to the highest percent passing. The blasting on the second day has the lowest percent passing, while the blasting on the fifth day has the highest percent passing. Blastings that are connected by a line shows that the percent passing do not have a significant difference. For example, the blastings on the second, third, and seventh day have similar percent passing. To obtain a clearer picture, Table 11 presents the sequence of blasting based on the lowest to the highest percent passing for each grain size.

Table 11 Sequence of blasting based on the lowest to the highest percent passing

Grain Size	Blasting							
20 cm	7	2	3	5	1	6	4	8
40 cm	3	2	7	6	5	1	4	8
60 cm	2	3	7	6	8	1	4	5
80 cm	2	3	6	7	4	8	1	5
100 cm	2	4	8	3	6	7	5	1

4.0 CONCLUSION

The analysis result shows that there is no significant difference in percent passing by Kuz-Ram method and percent passing by Split Desktop. Even though the difference is not significant, it cannot be denied that there is indeed a difference in both percentage passing values. With the analysis that has been done, the calibration is:

- Split = Kuz-Ram + 7.533 for grain size of 20 cm
- Split = Kuz-Ram - 2.113 for grain size of 40 cm
- Split = Kuz-Ram - 5.279 for grain size of 60 cm
- Split = Kuz-Ram - 1.965 for grain size of 80 cm
- Split = Kuz-Ram + 7.829 for grain size of 100 cm

The values above show that the differences of percent passing values by Kuz-Ram and Split Desktop vary for each grain size. Percent passings for grain sizes of 40 cm and 80 cm have good accuracy, with the error value of around 2%. For the other grain sizes, the error ranges approximately from 5% to 7%. Overall, the Kuz-Ram method has fairly good accuracy in predicting fragmentation of andesitic rocks.

Conflicts of Interest

The author(s) declare(s) that there is no conflict of interest regarding the publication of this paper.

Acknowledgement

The author would like to thank the management of PT AB Omah Geo for supporting this research.

References

[1] Hekmat, A., Munoz, S., and Gomez, R. 2019. Prediction of Rock Fragmentation Based on A Modified Kuz-Ram Model. *Proceedings of the 27th International Symposium on Mine Planning and Equipment Selection - MPES 2018*. 69-79. Doi: http://dx.doi.org/10.1007/978-3-319-99220-4_6.

[2] Gheibie, S., Aghababaei, H., Hoseinie, S. H., and Pourrahimian, Y. 2009. Modified Kuz—Ram Fragmentation Model and Its Use at The Sungun Copper Mine. *International Journal of Rock Mechanics and Mining Science*. 46: 967-973. Doi: http://dx.doi.org/10.1016/j.ijrmms.2009.05.003.

[3] Akbari, M., Lashkaripour, G., Bafghi, A. Y., and Ghafoori, M. 2015. Blastability Evaluation for Rock Mass Fragmentation in Iran Central Iron Ore Mines. *International Journal of Mining Science and Technology*. 25(1): 59-66. Doi: http://dx.doi.org/10.1016/j.ijmst.2014.11.008.

[4] Mutinda, E. K., Alunda, B. O., Maina, D. K., and Kasomo, R. M. 2021. Prediction of Rock Fragmentation Using the Kuznetsov-Cunningham-Ouchterlony Model. *Journal of the Southern African Institute of Mining and Metallurgy*. 121(3):107-112. Doi: http://dx.doi.org/10.17159/2411-9717/1401/2021.

[5] Han, J-H., and Song, J-J. 2014. Statistical Estimation of Blast Fragmentation by Applying Stereophotogrammetry to Block Piles. *International Journal of Rock Mechanics and Mining Sciences*. 68: 150-158. Doi: http://dx.doi.org/10.1016/j.ijrmms.2014.02.010.

[6] Elahi, A. T., and Hosseini, M. 2017. Analysis of Blasted Rocks Fragmentation Using Digital Image Processing (Case Study: Limestone Quarry of Abyek Cement Company). *International Journal of Geo-Engineering*. 8: 16. Doi: http://dx.doi.org/10.1186/s40703-017-0053-z.

[7] Souza, J. C. d., Silva, A. C. S. d., and Rocha, S. S. 2018. Analysis of Blasting Rocks Prediction and Rock Fragmentation Results Using Split-Desktop Software. *Tecnologia em Metalurgia, Materiais e Mineração*. 15(1): 22-30. Doi: http://dx.doi.org/10.4322/2176-1523.1234.

[8] Idowu, K. A., Olaleye, B. M., and Saliu, M. A. 2021. Application of Split Desktop Image Analysis and Kuz-Ram Empirical Model for Evaluation of Blast Fragmentation Efficiency in A Typical Granite Quarry. *Ghana Mining Journal*. 21(1): 45-52. Doi: http://dx.doi.org/10.4314/gm.v21i1.5.

[9] Jug, J., Strelec, S., Gazdek, M., and Kavur, B. 2017. Fragment Size Distribution of Blasted Rock Mass. *IOP Conference Series: Earth and Environmental Science*. 95(4): 042013. Doi: http://dx.doi.org/10.1088/1755-1315/95/4/042013.

[10] Azadmehr, A., Jalali, S. M. E., and Pourrahimian, Y. 2019. An Application of Rock Engineering System for Assessment of The Rock Mass Fragmentation: A Hybrid Approach and Case Study. *Rock Mechanics and Rock Engineering*. 52: 4403-4419. Doi: http://dx.doi.org/10.1007/s00603-019-01848-y.

[11] Tao, J., Yang, X-G., Li, H-T., Zhou, J-W., Qi, S-C., and Lu, G-D. 2020. Numerical Investigation of Blast-Induced Rock Fragmentation. *Computers and Geotechnics*. 128: 103846. Doi: http://dx.doi.org/10.1016/j.compgeo.2020.103846.

[12] Zhang, Z-X., Hou, D-F., Guo, Z., He, Z., and Zhang, Q. 2020. Experimental Study of Surface Constraint Effect on Rock Fragmentation by Blasting. *International Journal of Rock Mechanics and Mining Sciences*. 128: 104278. Doi: http://dx.doi.org/10.1016/j.ijrmms.2020.104278.

[13] Zhang, Z-X., Qiao, Y., Chi, L. Y., and Hou, D-F. 2021. Experimental Study of Rock Fragmentation Under Different Stemming Conditions in Model Blasting. *International Journal of Rock Mechanics and Mining Sciences*. 143: 104797. Doi: http://dx.doi.org/10.1016/j.ijrmms.2021.104797.

[14] Balakrishnan, V., Pradhan, M., and Dhekne, P. Y. 2019. Investigating Rock Fragmentation in Distributed Spherical Air-Gap Blasting Technique. *Powder Technology*. 362: 101-110. Doi: http://dx.doi.org/10.1016/j.powtec.2019.11.110.

[15] Yan, P., Zhou, W., Lu, W., Chen, M., and Zhou, C. 2016. Simulation of Bench Blasting Considering Fragmentation Size Distribution. *International Journal of Impact Engineering*. 90: 132-145. Doi: http://dx.doi.org/10.1016/j.ijimpeng.2015.11.015.

[16] Navarro, J., Seidl, T., Hartlieb, P., Hartlieb, P., Sanchidrián, J. A., Segarra, P., Couceiro, P., Schimek, P., and Godoy, C. 2021. Blastability and Ore Grade Assessment from Drill Monitoring for Open Pit Applications. *Rock Mechanics and Rock Engineering*. 54: 3209-3228. Doi: http://dx.doi.org/10.1007/s00603-020-02354-2.

[17] Sanchidrián, J. A., and Ouchterlony, F. 2017. A Distribution-Free Description of Fragmentation by Blasting based on Dimensional Analysis. *Rock Mechanics and Rock Engineering*. 50: 781-806. Doi: http://dx.doi.org/10.1007/s00603-016-1131-9.

[18] Segarra, P., Sanchidrián, J. A., Navarro, J., and Castedo, R. 2018. The Fragmentation Energy-fan Model in Quarry Blasts. *Rock Mechanics and Rock Engineering*. 51: 2175-2190. Doi: http://dx.doi.org/10.1007/s00603-018-1470-9.

[19] Lawal, A. I. 2021. A New Modification to The Kuz-Ram Model Using the Fragment Size Predicted by Image Analysis. *International Journal of Rock Mechanics and Mining Sciences*. 138: 104595. Doi: http://dx.doi.org/10.1016/j.ijrmms.2020.104595.

[20] Morin, M. A., and Ficarazzo, F. 2006. Monte Carlo Simulation as a Tool to Predict Blasting Fragmentation Based on The Kuz–Ram Model. *Computers & Geosciences*. 32(3): 352-359. Doi: http://dx.doi.org/10.1016/j.cageo.2005.06.022.

[21] Faramarzi, F., Mansouri, H., and Farsangi, M. A. E. 2013. A Rock Engineering Systems based Model to Predict Rock Fragmentation by Blasting. *International Journal of Rock Mechanics and Mining Sciences*. 60: 82-94. Doi: http://dx.doi.org/10.1016/j.ijrmms.2012.12.045.

[22] Ebrahimi, E., Monjezi, M., Khalesi, M. R., and Armaghani, D. J. 2016. Prediction and Optimization of Back-Break and Rock Fragmentation using an Artificial Neural Network and a Bee Colony Algorithm. *Bulletin of Engineering Geology and the Environment*. 75: 27-36. Doi: http://dx.doi.org/10.1007/s10064-015-0720-2.

[23] Lilly, P. A. 1986. An Empirical Method of Assessing Rock Mass Blastability. *Proceedings of the Large Open Pit Mining Conference*. 89-92.

[24] Kuznetsov, V. M. 1973. The Mean Diameter of the Fragments Formed by Blasting Rock. *Soviet Mining Science*. 9: 144-148. Doi: http://dx.doi.org/10.1007/bf02506177.

[25] Ouchterlony, F., and Sanchidrián, J. A. 2019. A Review of Development of Better Prediction Equations for Blast Fragmentation. *Journal of Rock Mechanics and Geotechnical Engineering*. 11(5): 1094-1109. Doi: http://dx.doi.org/10.1016/j.jrmge.2019.03.001.

[26] Supandi, Zakaria, Z., Sukiyah, E., and Sudradjat, A. 2018. The Correlation of Exposure Time and Claystone Properties at The Warukin Formation. *International Journal of GEOMATE*. 15(52): 160-167. Doi: http://dx.doi.org/10.21660/2018.52.68175.

[27] Supandi, Zakaria, Z., Sukiyah, E., and Sudradjat, A. 2020. New Constants of Fracture Angle on Quartz Sandstone. *International Journal on Advanced Science, Engineering and Information Technology*. 10(4): 1597-1603. Doi: http://dx.doi.org/10.18517/ijaseit.10.4.8272.

[28] Sujatono, S. 2022. Geological, Geomechanical and Geochemical Analysis on Claystone of the Sebamban Syncline. *Geotechnical and Geological Engineering*. 40: 2145-2155. Doi: http://dx.doi.org/10.1007/s10706-021-02017-1.

[29] Supandi, Zakaria, Z., Sukiyah, E., and Sudradjat, A. 2019. The Influence of Kaolinite-Illite Toward Mechanical Properties of Claystone. *Open Geosciences*. 11(1): 440-446. Doi: http://dx.doi.org/10.1515/geo-2019-0035.

[30] Sudjana. 2002. *Desain dan Analisis Eksperimen*. Bandung: Tarsito.